Pure Appl. Chem., Vol. 83, No. 9, pp. 1751–1762, 2011.
doi:10.1351/PAC-CON-10-11-14

Peptide models in the study of the mechanism of carcinogenesis by heavy metals*

Gerasimos Malandrinos, Ana-Monica Nunes, Kimon Zavitsanos, and Nick Hadjiliadis‡

Department of Chemistry, University of Ioannina, 45110 Ioannina, Greece

Abstract: The molecular mechanisms of carcinogenesis involving heavy metal ions are not yet fully understood. Histones surrounding DNA are believed to be primary targets for metal ion binding, and such interactions may play a direct or indirect role in metal-induced toxicity carcinogenesis. This paper reviews our results of approximately the last 10 years in this area, starting from small peptide fragments and models of various histones and ending with longer ones. It was found that almost all peptide models reacted strongly with metal ions, and in some cases the peptides in the presense of Cu(II) or Ni(II) were hydrolyzed. Oxidation of deoxyguanosine to 8-oxo-deoxyguanosine under physiological pH values was also observed in the presense of mild oxidation agents like H_2O_2 and certain metal ion–peptide complexes. With longer peptide chain models, a DNA strand breakage analysis was also carried out, indicating an increased DNA damage by Cu^{2+}/H_2O_2 and Ni^{2+}/H_2O_2 reaction mixtures. The results lead to proposals of possible mechanistic pathways of carcinogenesis caused by Cu(II) and Ni(II).

Keywords: carcinogenesis; copper(II); histone models; nickel(II); peptides.

INTRODUCTION

Histones are highly basic proteins that provide scaffold for DNA double helix in eukaryotic cell nuclei. It is well known that about 146 DNA base pairs are wrapped around a histone octamer which contains two copies of each of histones H2A, H2B, H3, and H4, forming the nucleosomes [1,2]. The repeated nucleosomes are further organized to highly and more condensed structures called chromatins.

The five most important types of histones are H1 (DNA linker histone), H2A, H2B, H3, and H4. Two copies of H2A, H2B, H3, and H4 are forming the histone octamer while H1 is located outside the nucleosome core and binds DNA [1,2]. It should be noted that N- and C-terminal tails of histones are the major but not the only interaction sites with DNA.

Seeking for the possible metal binding sites inside the cell nucleus may provide the molecular basis for a better understanding of the interactions responsible for cancer or similar genetic disease developments. DNA and/or histones metal ion's interaction may have repercussions in the genetic code. The plenitude of histones in the nucleosome core makes them excellent candidates for binding metal ions. Metal ions may induce toxicity-carcinogenesis by oxidative or non-oxidative pathways. In the first case, it is proposed that metal ions are able to activate O_2 or mild oxidants such as H_2O_2 and produce superoxide and/or hydroxyl radicals through Fenton/Haber-Weiss type reactions. These active oxygen

*Paper based on a presentation made at the 11th Eurasia Conference on Chemical Sciences, The Dead Sea, Jordan, 6–10 October 2010. Other presentations are published in this issue, pp. 1643–1799.

‡Corresponding author

species can then interact with DNA leading to strand scission, depurination, cross-linking, DNA-bases modification, etc., affecting the genetic code and causing cancer [3,4]. On the other hand, direct binding of metal ions to histones and/or DNA could intervene with nucleosome structure and organization due to structural changes that are normally expected to occur or in some cases metal-mediated hydrolysis, while binding to or close to histone methylation, acetylation, phosphorylation, and ubiquination sites may alter the histone code, which in turn is linked with important biological pathways involving the cell nucleus such as gene expression, DNA repair mechanisms, and others [5–8].

Detection and chemical and structural description of specific metal binding sites would provide the molecular basis for better understanding of the effects that eventually lead to cancer development. In this respect, previous studies have shown that certain histone peptide models, fragments of H2A, H2B, H3, and H4, may serve as efficient binding sites for metal ions such as Cu(II) and Ni(II) [9–15]. Moreover, interactions of metal ions with small peptides have revealed that His residues are the major coordination sites of several transition-metal ions, including Ni(II) and Cu(II), in proteins [16–19].

In this paper, we briefly review our research results in this area during the last few years. We have synthesized various histone models (N- and C-terminal protected) and studied their interactions using various physico-chemical techniques, including UV–vis, EPR, NMR, CD, potentiometric titrations, etc. The first peptides chosen included the hexapeptide models of the -ESHH- motif of the C-terminal histone H2A (residues 121–124) [20–25]. We continued with the peptides -ELAKHA- [26], -LAHYNK- [27], and -TYTEHAK- [28] models of histones H2B and H4, respectively (residues 102–107, 80–85, and 71–76). Very recently, models of histone H2B (residues 1–31, 32–62, 63–93, and 94–125) were evaluated as well [29–33].

SMALL PEPTIDE MODELS

Our work in this interesting area was initiated by synthesizing a series of peptides, i.e., -TESHHK-, -TASHHK-, -TEAHHK-, -TESAHK-, -TESHAK-, SHHK, SAHK modeling the -ESHH- motif of the C-terminal histone H2A (residues 121–124) [20–26]. It was earlier observed [12,13] that at pH ~7.4 the peptide Ac-TESHHK-amide underwent Ni(II)-assisted hydrolysis of E–S bond resulting in a more stable Ni(II)-SHHK-amide complex. Study of the coordination and hydrolytic properties of the above models towards Ni(II) and Cu(II) ions was expected to give answers concerning (a) the effects of Glu and Ser substitution on the stability of the complexes formed, (b) the amino acid(s) responsible for hydrolysis, and (c) better understanding of the hydrolysis mechanism. Besides the rich coordination chemistry of the peptides described in detail [12,13,20–25], we found that only the sequences containing an amino acid with a hydroxyl group near the coordination site, namely, at the third position like Ser or Thr, in the presence of Ni(II) at pH ~7.4, were hydrolyzed (Fig. 1). The His residue at position five, proved to be always linked with Ni(II) ions, is also important. The driving force for hydrolytic cleavage is the very high stability of the resulting complexes with sequences -SHHK- or -SAHK- produced by hydrolysis. Based on the above results, a mechanism was proposed in which a possible hydrogen bond formed between the hydroxyl group of the Ser residue and the glutamic or alanine carbonyl oxygen was assumed to be essential for increasing the positive charge on the carbon atom of Glu or Ala residue and making it more sensitive to nucleophilic attack by hydroxyl or water molecules [22]. Later the peptide Ac-TETHHK-amide was found to undergo a similar hydrolytic reaction [34], highlighting the importance of Thr residue at position 3 or in general the presence of alcoholic –OH groups at the proper position. Very recently, a slightly different mechanism of Ni(II)-assisted hydrolysis of a series of peptides in the general sequence R1-(Ser/Thr)-Xaa-His-Zaa-R2 (Xaa, Zaa = any amino acid) was presented [35]. Following the formation of a 4N square planar Ni(II) complex, a N–O acyl shift was proposed yielding an intermediate ester with Ser (or Thr) alcoholic group. This ester was then hydrolyzed, yielding the final products.

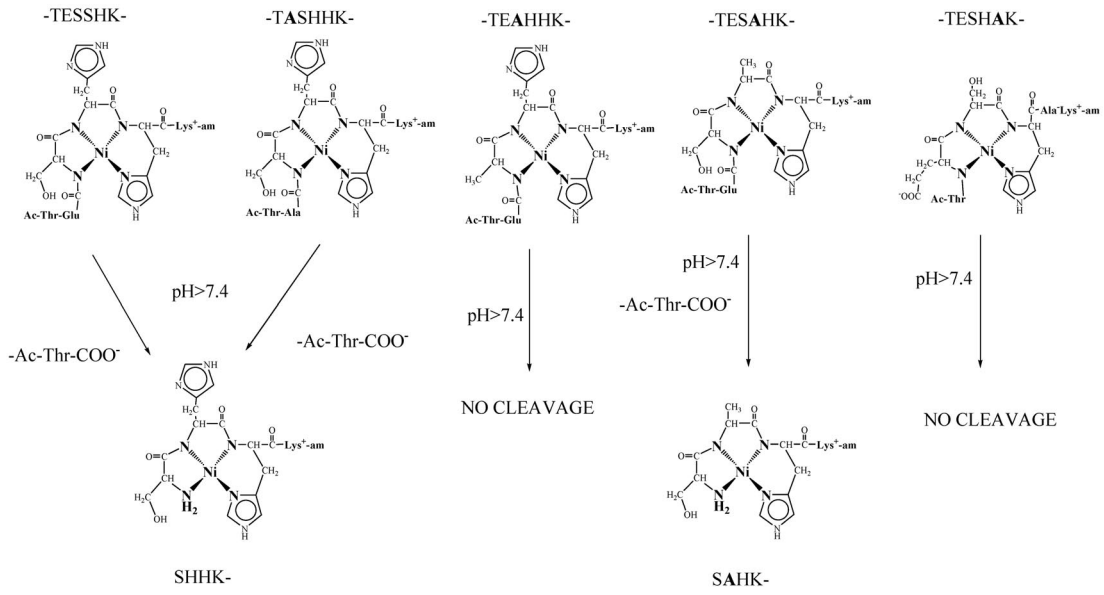

Fig. 1 Hydrolytic properties of a series of peptides modeling the -SHHK- sequence.

The oxidative ability of Cu-TESHHK complex at physiological pH was checked as well. Under these conditions, Cu(II) is coordinated through the imidazole nitrogen of His-4 residue, the amide nitrogens of Ser-3 and His-4 while His-5 imidazole occupies an equatorial position. This complex was found to activate H_2O_2 and efficiently oxidized 2'-deoxyguanosine to 8-oxo-deoxyguanosine. The redox reaction involved a Cu(III) species and a metal-bound hydroxyl radical finally yielding a superoxide radical which eventually oxidized 2'-deoxyguanosine [20].

The next two peptide sequences studied included Ac-TYTEHA-amide and Ac-LAHYNK-amide models of histones H4 and H2B (residues 71–76 and 80–85), respectively [27,28]. It was found that Cu(II) and Ni(II) ions form relatively stable complexes with the peptide Ac-TYTEHA-amide over the pH range 3.5–11. His imidazole acted as an anchor site for both ions while the successive deprotonation and coordination of amide donors saturated the equatorial coordination plane (Fig. 2). In addition, Ni(II)-mediated hydrolysis of the peptide bond Tyr-Thr was observed (Fig. 3), yielding the fragments Ac-TY-COO^- and H_2N-TEHA-amide supporting our earlier findings underlying the requirement of a Ser or Thr residue near the coordination sites for the hydrolysis to occur.

The -LAHYNK- sequence studied next [27] presents the typical binding motifs of peptides having a His residue in an internal position with both metal ions. In this case, it is interesting to note the very high stability of the Cu(II) complex formed in neutral media presenting a $\{N_{imidazole}, 2N_{amide}\}$ binding motif and accounting for almost 98 % of the total metal ion concentration at pH 7.3. This strongly indicates that at physiological pH values the sequence -LAHYNK- of histone H2B provides very efficient binding sites for metal ions. The imidazole pyrrole N(1) ionization (but not coordination) was also detected in species present in solution above pH ~11. Hydrolysis of the peptide in the presence of Ni(II) ions was not observed in this case, as no Ser or Thr residues are present in the studied sequence.

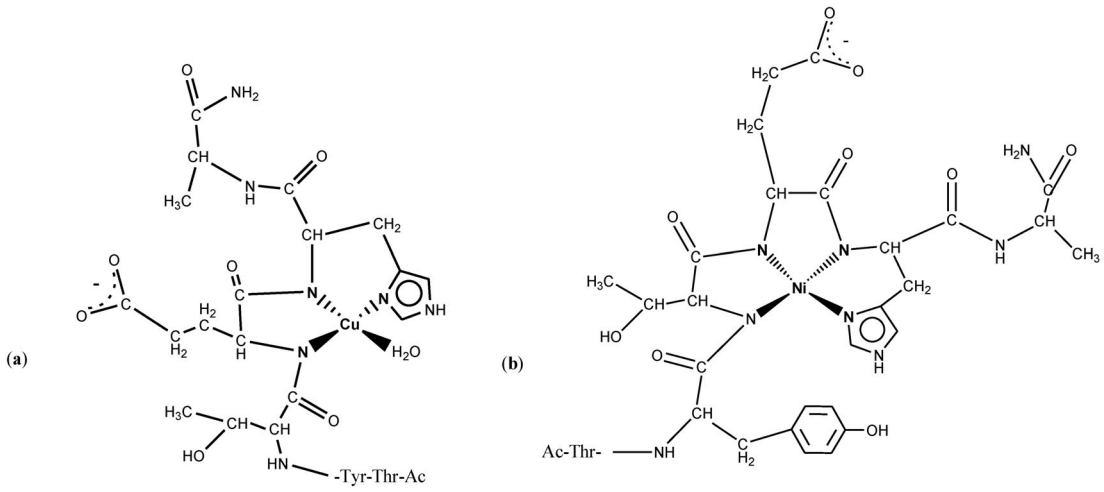

Fig. 2 Cu(II) and Ni(II) complexes with Ac-TYTEHA-amide. (a) Cu(II) complex present at neutral pH, (b) Ni(II) complex predominant at pH ~9.5.

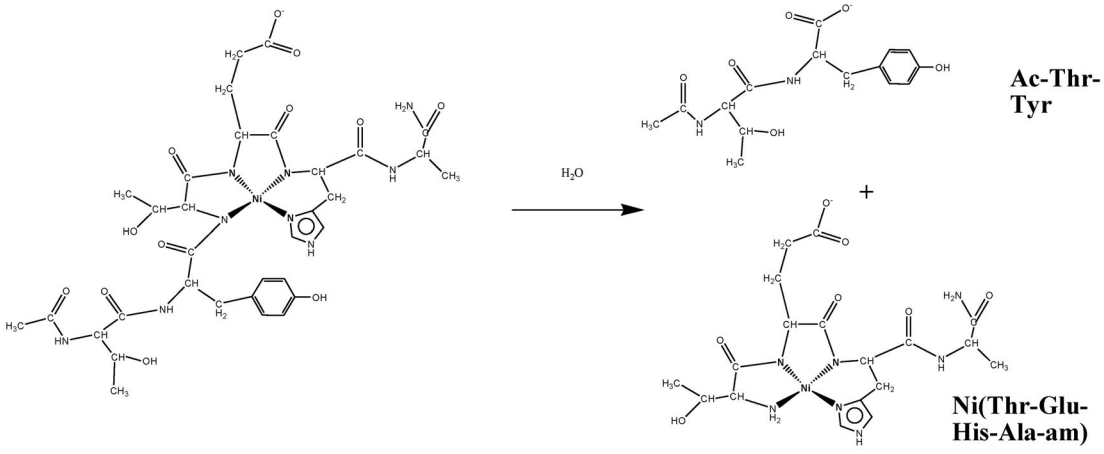

Fig. 3 The hydrolysis reaction observed in Ni(II)-Ac-TYTEHA-amide system.

Briefly, the main conclusions drawn from our studies with small peptide models are:

(a) All peptide models interact strongly with the metal ions over the pH range 5–10.5. The imidazole side chain of His is the initial metal anchoring group while successive coordination of amide donors saturate the equatorial plane leading to 4N complexes above pH ~9.

(b) Peptide hydrolytic cleavage in the presence of metal ions was observed only when Ser or Thr residues were located near the coordination sites.

(c) The Cu-TESHHK complex formed at physiological conditions (pH = 7.4 and T = 310 K) efficiently promoted oxidation of 2'-deoxyguanosine, with transient formation of substantial amounts of 8-oxo-deoxyguanosine.

LONGER PEPTIDE MODELS

Our next challenge was to synthesize longer peptide chain models. In this respect, we decided to divide histone H2B into four 30-31mer fragments and eventually synthesize the corresponding peptides shown in Fig. 4. Their interaction with Cu(II) and Ni(II) ions was then studied by means of spectroscopic techniques (polynuclear and multidimensional NMR, EPR, UV–vis, etc.) and potentiometric titrations. In addition, a DNA strand breakage analysis was also carried out under specific conditions.

Peptide (1): ($H2B_{1\text{-}31}$)
Acetyl-PEPAKSAPAPKKGSKKAVTKAQKKDGKKRKR-amide
peptide (2): ($H2B_{32\text{-}62}$)
Acetyl-SRKQSYSVYVYKVLKQVHPDTGISSKAMGIM-amide
peptide (3): ($H2B_{63\text{-}93}$)
Ac-NSFVNDIFERIAGEASRLAHYNKRSTITSRE-amide
peptide (4): ($H2B_{94\text{-}125}$)
Ac-IQTAVRLLLPGELAKHAVSEGTKAVTKYTSSK-amide

Fig. 4 Synthesized peptides modeling histone H2B.

$H2B_{1–31}$–Cu(II), Ni(II) interaction

The first peptide studied [31] corresponded to 1–31 residues of the N-termini tail of histone H2B (Acetyl-PEPAKSAPAPKKGSKKAVTKAQKKDGKKRKR-amide). This was the only sequence in which potentiometric measurements were not carried out due to the absence of nitrogen anchors for metal ions neither at N-terminal or side chains (His imidazole). The absence of a strong coordination residue in $H2B_{1–31}$ peptide made extremely difficult an accurate determination of its metal binding sites. Nevertheless, the spectroscopic results indicate that Cu^{2+} starts binding to $H2B_{1–31}$ above pH 7.3, most probably through the β-carboxylate group of D25. Above pH 8.5, there is a mixture of 3N $\{N^-_{D25}$, N^-_{K24}, CO, $\varepsilon NH_2\}$ and 4N $\{N^-_{D25}$, N^-_{K24}, OH_2, $\varepsilon NH_2\}$ $\{\ \varepsilon NH_2\}$ (N^- = amide donors) species with two deprotonated amides equatorially coordinated to Cu^{2+}. Increase of the pH, over 10, results in water molecule substitution by the β-carboxylate of D25 while in more basic media deprotonation and coordination of an additional amide donor occurs $\{N^-_{D25}$, N^-_{K24}, N^-_{K23}, $\varepsilon NH_2\}\{\beta\text{-}COO^-\}$. Ni(II) coordination not as effective as Cu(II) was detected at pH ~6.7 most probably involving the β-carboxylate of D25 residue. At higher pH values, NMR spectroscopy supports the involvement of Q22-K23-K24-D25 fragment in direct coordination to Ni^{2+}, in a $\{4N^-\}$ coordination mode. It is also interesting to note that 2D NMR showed a structural rearrangement in $H2B_{1–31}$ upon Ni^{2+} complexation, affecting mostly the residues G13-S14-K15-K16-A17-V18-T19-K20-A21-Q22-K23-K24-D25-G26. The proposed structures of some of the complexes discussed above are presented in Fig. 5.

H2B N-termini tail residues K15, K23, and K27 are acetylation sites, and S14 is where phosphorylation takes place [36,38]. Metal binding or conformation alteration of the fragment G13—G26 evident from our results, might present severe biological consequences due to disruption of these post-translational modifications, causing neoplastic transformation in cells.

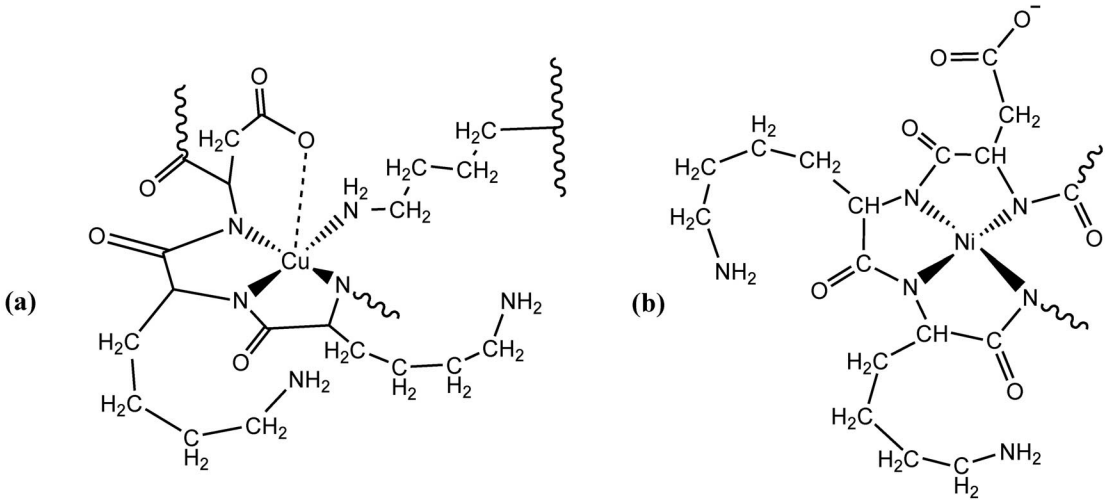

Fig. 5 Cu(II), Ni(II)–$H2B_{1–31}$ complexes. (a) Proposed structure of a 4N Cu(II) complex with equatorial binding of Asp β-carboxylate formed at highly basic media. (b) Proposed structure of the Ni(II) 4N complex.

$H2B_{32–62}$–Cu(II) interaction

The peptide $H2B_{32-62}$ (Acetyl-SRKQSYSVYVYKVLKQVHPDTGISSK-AMGIM-amide) represents the N-terminal fold domain of histone H2B. The free peptide precipitates over pH ~7.8 and redissolves in the presence of Cu(II) ions only. Therefore, the study could not be completed with Ni(II). The explanation that may be given to the precipitation of the free peptide at pH ~7.9, may involve the adoption of a secondary structure leading to charge neutralization. Cu(II) binding results in changes of ligand conformation while offering extra charges to the molecule leading to solubility enhancement. The binding of the $H2B_{32–62}$ peptide with Cu(II) ions is quite efficient. Several soluble Cu(II) complexes were detected in the pH range 4–10.5. At physiological pH, two major complexes are formed, where Cu(II) binds to the peptide in a 3N $\{N_{Imidazole}, 2N^{-}\}$ mode. These species are coordination isomers. The only difference between them is that in one, the carboxylate group of the Asp_{20} binds in an axial position (Fig. 6). A possible explanation for the existence of these isomers is that the presence of Pro49 residue in the peptide's primary structure creates a breakpoint and induces the adoption of a structure where Asp50 carboxyl group is located close to the metal ion.

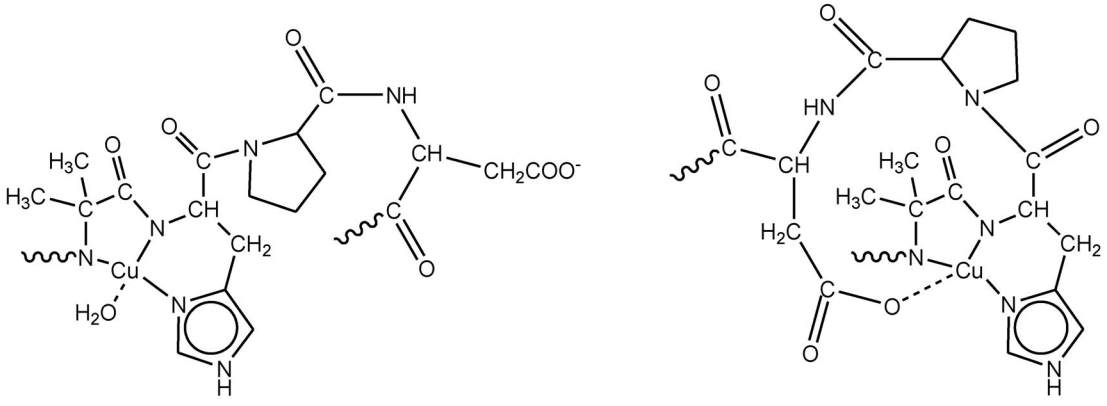

Fig. 6 Proposed structures of the 3N Cu(II) coordination isomers formed at neutral pH (system Cu(II)–$H2B_{32–62}$).

While $H2B_{32–62}$ residues are not subject to covalent modifications (histone code), conformational changes of $H2B_{32–62}$ induced by Cu(II) coordination may interfere with the dynamic nature of the nucleosome or alter the octamer's structure. Additionally, residues 30–37 of H2B are considered to be essential for DNA repair systems [39], and thus any chemical or structural alteration will influence the efficiency of DNA repair mechanisms.

$H2B_{63–93}$–Cu(II), Ni(II) interaction

The next peptide synthesized was the fragment 63–93 of the central part of H2B histone-fold domain ($H2B_{63–93}$) (Acetyl-NSFVNDIFERIAGEASRLAHYNK-RSTITSRE-amide). Based on NMR data in solution, we found that the peptide adopts two well-defined structural elements: an α-helix from G13 up to H20 and a possible β-strand for the T26-I27-T28 segment. These data indicate a structural similarity between the synthesized peptide and the actual fragment of the histone, situated in the nucleosome core. The crystal structure of the nucleosome [40] shows this motif to adopt an α-helix structure from residue 1–22 and a loop from 23–28, containing a β-sheet at T26-I27. This is of particular interest for the helical region since it incorporates the metal binding site. Hence, we believe $H2B_{63–93}$ to be a consistent model of 63–93 residues of H2B histone-fold domain. Acetyl-NSFVNDIFERIAGEASR-LAHYNKRSTITSRE-amide binds Ni^{2+} and Cu^{2+} ions efficiently. Potentiometric and spectroscopic studies (UV–vis, CD, and EPR) showed that His_{21} imidazole nitrogen acts as an anchoring donor for the metal ions. At physiological pH values, 3N species $\{N_{Imidazole}, 2N^-\}$ are detected while in basic pH values additional amide deprotonation and coordination yields 4N $\{N_{Im}, 3N^-\}$ complexes. Ni^{2+} binding with the $H2B_{63–93}$ involves several species formed starting from distorted octahedral mono or bidentate at about neutral pH, to a square planar complex where the peptide is bound through a $\{N_{Imidazole}, 3N^-\}$ mode in equatorial plane at basic pH values [29,30] (Fig. 7). Multidimensional NMR spectroscopy confirmed the proposed binding mode of $H2B_{63–93}$-Ni^{2+} species, with the coordination involving the imidazole of His_{20} and three amide nitrogens of His_{20}, Ala_{19}, and Leu_{18}. The solution structure of the Ni^{2+} complex with the tridecapeptide comprising histone's H2B 75–87 residues, was

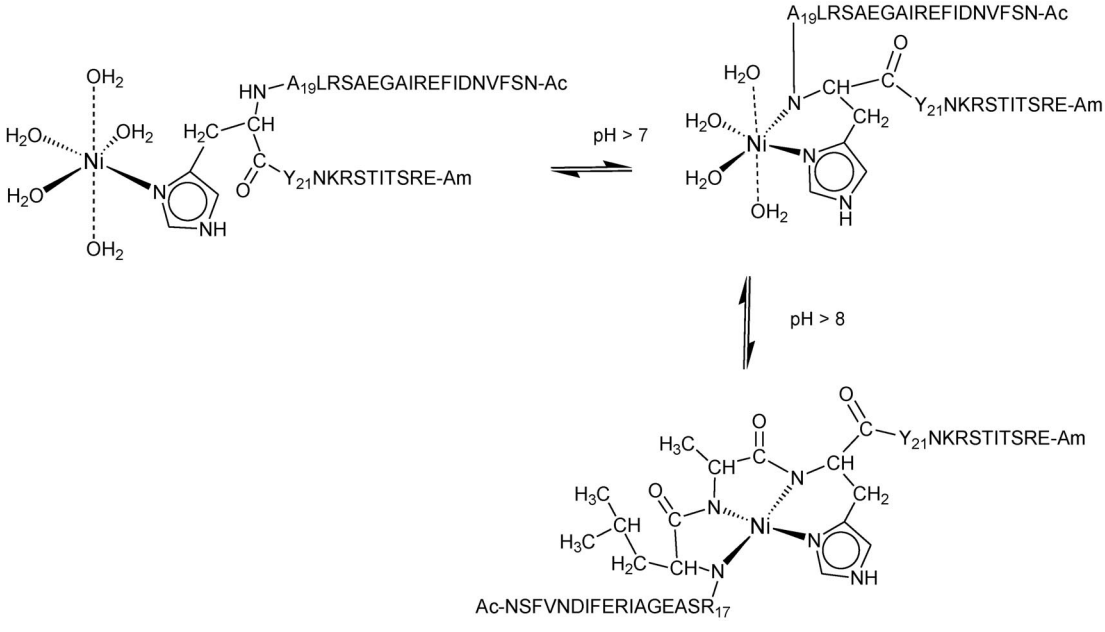

Fig. 7 Structural variation of Ni(II)–$H2B_{63–93}$ complexes vs. pH.

elucidated from the nuclear Overhauser effect (NOE) cross-correlations observed in the 2D-NOESY spectrum. The structure showed a severe change in the peptide's conformation, passing from a partially helical to a well-defined ordered structure around the metal ion. Other important features derived from this fragment structure analysis were (i) the location of the Tyr83 aromatic ring near the nickel coordination site, indicating a possible interaction of the negative partial charge of the phenolic oxygen with the positive part of the electrostatic potential generated by the nickel complex; (ii) the formation of an axial hydrophobic fence (side chains of Leu80 and Ala81), shielding one side of the coordination plane from the bulk of the solution; (iii) the arrangement of the Arg_{86} side chain near the Tyr_{83} ring in a tilted parallel equatorial position to the coordination plane and to the Arg_{79} side chain (Fig. 8). All these residues seem to shield the coordination plane from the solvent water molecules, increasing complex stability [30].

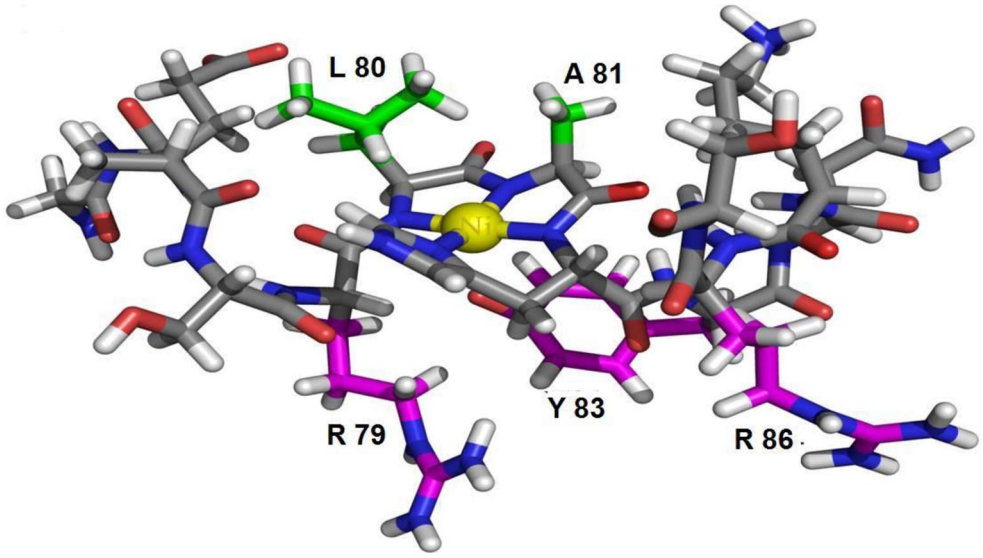

Fig. 8 Solution structure of the Ni^{2+} complex with the tridecapeptide comprising histone's H2B 75–87 residues derived from NMR data.

Residues Arg_{82}, Tyr_{83}, Thr_{88}, Glu_{93}, and Arg_{86} are involved in hydrophobic interactions or hydrogen bonds with other histones (H2A, H3, and H4) and DNA phosphate groups [1,40]. Therefore, structural modifications observed for $H2B_{63–93}$ as a consequence of metal ion binding may have a great impact on nucleosome structure and dynamics.

$H2B_{94–125}$–Cu(II), Ni(II) interaction

Our coordination studies towards histone peptides models were completed with C-terminal fragment of H2B (residues 94–125, Acetyl-IQTAVRLLLPGELAKHAVSEGTKAVTKYTSSK-amide). The peptide incorporates a part of the α3 helix of the histone fold domain and the C-terminus. This part of histone H2B is accessible to metal ions and offers most likely binding sites within the protein [1]. It is also involved in important biological processes, such as ubiquitination of K120 which in turn mediates histone H3 K4 residue methylation responsible for preventing cell silencing, DNA transcription activation, and formation of higher-order chromatin structure [41,42].

Ni(II) interaction with $H2B_{94–125}$ yielded several species over the pH range 5–11. Low-spin diamagnetic complexes started to form above pH 9 while no free Ni(II) exists in solution above pH 10. The

formation of the square planar complex with 4N $\{N_{Imidazole}, 3N^-\}$ binding mode was further studied by means of NMR spectroscopy (pH 10) and a solution structure for the Ni(II) complex with the fragment $-Glu_{12}$-Leu_{13}-Ala_{14}-Lys_{15}-His_{16}-Ala_{17}-Val_{18}-Ser_{19}- was elucidated from the NOE cross-correlations, observed [33]. Unfortunately, the lack of meaningful NOEs did not allow us to determine the structure of the complex with the whole peptide sequence. However, there is evidence that complexation affects the C-terminal of the peptide, as well, leading to a structure where this fragment approaches the coordination plane. If such a structural alteration may occur under physiological conditions, it is highly possible to interfere with the ubiquitination process of Lys_{120}. The solution structure revealed also a few more interesting features. The backbone of Ala_{110}, Val_{111}, and Ser_{112} is placed over the metal coordination plane while the hydrophobic side chains of Ala_{110} and Val_{111} and the bulky aliphatic group of Leu_{106} are positioned below it. These residues act as a shield to the coordination site from the bulk of the solution and thus enhance the stability of the 4N complex.

$H2B_{94–125}$ is an efficient target for Cu(II) binding as well. Potentiometry detects the formation of several species in the pH range 4–11.5. At physiological pH the major species is a 3N complex where Cu(II) ions bind through a $\{N_{Imidazole}, 2N^-\}$ mode. 4N complexes predominate in the alkaline region. It should be noted that although the peptides $H2B_{94–125}$ and -ELAKHA- studied earlier [26] share the same binding site Ala-Lys-His, with Cu(II), the first one forms more stable complexes than the second. This may be attributed either to side-chain interactions and/or induction of a secondary structure.

DNA strand breakage analysis

Our studies were focused thus far on the coordination behavior of small and longer histone peptide models. We have presented evidence about the influence that metal coordination may have in terms of structural modifications. Possible consequences of these structural alterations upon metal binding in post-translational modifications, DNA repair mechanisms, and nucleosome dynamics (nonoxidative pathways) were also highlighted. Here we will refer briefly to a part of our results dealing with the study of the oxidative decomposition of DNA fragments in the presence of (a) Cu(II)-histone $H2B_{63–93}$, (b) Ni(II)-histone $H2B_{32–62}$ and a mild oxidant, such as H_2O_2. It should be reminded that both histone models are fragments of the histone H2B fold domain, and it is expected to interact strongly with DNA. The complete study and more details will be given elsewhere [43].

The ability of the peptide metal complexes to induce DNA double-strand breaks was studied with agarose gel electrophoresis, using the plasmid pUC19 as a target molecule under physiological conditions pH = 7.4, T = 310 K. In the first case mentioned above, an increase of double-strand scission of the plasmid was observed in the presence of $H2B_{63–93}$. The enhancement of DNA strand break relative to copper is more pronounced when the metal concentration reaches similar concentration with the peptide. These findings support the coordination of Cu^{2+} towards $H2B_{63–93}$. In fact, at this pH value, the peptide presents a high affinity towards Cu^{2+}, forming 80 % of 3N species, where the metal is coordinated to the imidazole nitrogen and two deprotonated amides from the peptide backbone. The neighboring residues of the binding site (Arg_{82}, Tyr_{83}, Thr_{88}, Glu_{93}, and Arg_{86}) will be in contact with the DNA, and bring the redox active complex closer to it. Consequently, the generation of hydroxyl radicals will get much closer to the DNA, causing a site-specific generation of reactive oxygen species (ROS) that is in turn associated with the formation of double-strand breaks [44,45]. In the second case, (Ni(II)-histone $H2B_{32–62}$), a different behavior was observed. It is generally known that Ni(II) ions cause only single-strand scissions and that direct binding of metal to DNA is not necessary for ROS generation [45] (generation in the bulk of the solution). On the contary, in the studied case we observed an enhancement of double-strand scission in the presence of $H2B_{32–62}$. In addition, decomposition of the plasmid in small fragments is less, indicating a protective role of the peptide. These two opposite effects may be explained taking into account the high affinity of this fragment towards DNA (DNA shielding from ROS generation). On the other hand, hydroxyl radicals produced by Ni^{2+} and H_2O_2 in

the bulk of the solution may attack the peptide protective layer oxidizing the two methionine residues present in the primary structure of the peptide. The first oxidation product is a sulfoxide [46]. However, such a compound might be further oxidized to produce peroxy- or alkyl-radicals [47] that in turn may cause double-strand scissions. The formation of sulfoxides under our experimental conditions is evident by the mass spectra recorded upon incubation of our sample solutions [43].

CONCLUSIONS

The conclusions extracted from our research in this area over the last few years are summarized below:

(i) Cu(II) and Ni(II) ions can form stable complexes with the histone H2B peptides all over the pH range 3.5–11. At low pH values, both ions interact with the imidazole N3 nitrogen atom while at physiological pH values (~7.4) very stable Cu(II) 3N complexes $\{N_{imidazole}, 2N^-\}$ are formed.
(ii) 4N $\{N_{imidazole}, 3N^-\}$ yellow-colored square planar diamagnetic Ni(II) species predominate over pH ~8.
(iii) No hydrolysis was observed, following coordination of the metals with all long peptides, in accordance with our previous findings, requiring a Ser or Thr amino acid to be present near the metal coordination site for the hydrolysis to take place.
(iv) All peptides, on the other hand, suffered severe conformational changes to accommodate the metal ions that may cause the induction of epigenetic and promutagenic effects, influencing the nearby DNA.
(v) Both metals are able to induce formation of ROS species and cause damage to DNA, when coordinated to all peptides. Single- and double-strand scissions are observed in the presence of the metals, the peptides, and mild oxidizing agents such as H_2O_2.
(vi) More stable complexes were formed with the longer peptide models, due to side-chain interactions, although the coordination sites involved the smaller peptide sequences, -LAHYNK-, -TESHHK-, -ELAKHA- contained in the longer sequences studied.
(vii) All Ni(II) complexes initially form paramagnetic metal complexes which convert to square planar ones at pH >8.

All these effects, either alone or in a synergistic way, may be the cause of toxicity and carcinogenicity caused by these metal ions.

Our work strongly supports the fact that histones may be the prime candidates for metal ion binding. Possible metal ion-mediated hydrolysis or oxidation of either histones or DNA as indicated in this study, together with secondary interactions detected with the longer peptides, could cause cleavage of the nucleosome core and/or DNA mutations leading to cancer.

REFERENCES

1. K. Luger, A. W. Mader, R. K. Richmond, D. F. Sargent, T. J. Richmond. *Nature* **389**, 251 (1997).
2. S. C. Elgin, J. L Workman. *Chromatin Structure and Gene Expression*, 2nd ed., Oxford University Press, New York (2000).
3. K. S. Kasprzak. "Oxidative DNA damage in metal-induced carcinogenesis", in: *Toxicology of Metals*, L. W. Chang (Ed.), **18**, 299 (1996).
4. A. Sigel, H. Sigel, R. K. O. Sigel (Eds.). *Nickel and its Surprising Impact in Nature*, John Wiley, Chichester, **2** (2007).
5. T. Kouzarides. *Cell* **128**, 693 (2007).
6. L. Broday, W. Peng, M. H. Kuo, K. Salnikow, M. Zoroddu, M. Costa. *Cancer Res.* **60**, 238 (2000).
7. F. Golebiowski, K. S. Kasprzak. *Mol. Cell. Biochem.* **279**, 133 (2005).
8. A. A. Karaczyn, F. Golebiowski, K. S. Kasprzak. *Chem. Res. Toxicol.* **18**, 1934 (2005).
9. W. Bal, J. Lukszo, M. Jezowska-Bojczuk, K. S. Kasprzak. *Chem. Res. Toxicol.* **8**, 683 (1995).

10. M. A. Zoroddu, L. Schinocca, T. Kowalik-Jankowska, H. Kozłowski, K. Salnikow, M. Costa. *Environ. Health Perspect.* **110**, 719 (2002).
11. M. A Zoroddu, T. Kowalik-Jankowska, H. Kozłowski, H. Molinari, K. Salnikow, L. Broday, M. Costa. *Biochim. Biophys. Acta* **1475**, 163 (2000).
12. W. Bal, J. Lukszo, K. Bialkowski, K. S. Kasprzak. *Chem. Res. Toxicol*. **11**, 1014 (1998).
13. W. Bal, R. Liang, J. Lukszo, S. H. Lee, M. Dizdaroglu, K. S. Kasprzak. *Chem. Res. Toxicol.* **13**, 616 (2000).
14. M.-A. Zoroddu, M. Peana, T. Kowalik-Jankowska, H. Kozłowski, M. Costa. *J. Chem. Soc., Dalton Trans*. **3**, 458 (2002).
15. M.-A. Zoroddu, M. Peana, S. Medici. *Dalton Trans*. **3**, 379 (2007).
16. H. Kozłowski, W. Bal, M. Dyba, T. Kowalik-Jankowska. *Coord. Chem. Rev*. **184**, 319 (1999).
17. H. Sigel, R. B. Martin. *Chem. Rev*. **82**, 385 (1982).
18. H. Kozłowski, T. Kowalik-Jankowska, M. Jezowska-Bojczuk. *Coord. Chem. Rev*. **249**, 2323 (2005).
19. I. Sovago, K. Osz. *Dalton Trans*. **32**, 3841 (2006).
20. M. Mylonas, G. Malandrinos, J. C. Plakatouras, N. Hadjiliadis, K. S. Kasprzak, A. Krezel, W. Bal. *Chem. Res. Toxicol*. **14**, 1177 (2001).
21. M. Mylonas, J. C. Plakatouras, N. Hadjiliadis, A. Krezel, W. Bal. *Inorg. Chim. Acta* **339**, 60 (2002).
22. M. Mylonas, A. Krezel, J. C. Plakatouras, N. Hadjiliadis, W. Bal. *J. Chem. Soc., Dalton Trans*. 4296 (2002).
23. M. Mylonas, J. C. Plakatouras, N. Hadjiliadis. *J. Chem. Soc., Dalton Trans*. **24**, 4152 (2004).
24. M. Mylonas, A. Krezel, J. C. Plakatouras, N. Hadjiliadis, W. Bal. *J. Mol. Liq*. **118**, 119 (2005).
25. M. Mylonas, J. C. Plakatouras, N. Hadjiliadis, K. D. Papavasileiou, V. S. Melissas. *J. Inorg. Biochem*. **99**, 637 (2005).
26. T. Karavelas, M. Mylonas, G. Malandrinos, J. C. Plakatouras, N. Hadjiliadis, P. Mlynarz, H. Kozłowski. *J. Inorg. Biochem*. **99**, 606 (2005).
27. K. Panagiotou, M. Panagopoulou, T. Karavelas, V. Dokorou, A. Hagarman, J. Soffer, R. Schweitzer-Stenner, G. Malandrinos, N. Hadjiliadis. *Bioinorg. Chem. Appl.* (2008), doi:10.1155/2008/257038.
28. T. Karavelas, G. Malandrinos, N. Hadjiliadis, P. Mlynarz, H. Kozłowski, M. Barsam, I. Butler. *Dalton Trans*. 1215 (2008).
29. K. Zavitsanos, A. M. P. C. Nunes, G. Malandrinos, C. Kallay, I. Sovago, V. Magafa, P. Cordopatis, N. Hadjiliadis. *Dalton Trans*. 6179 (2008).
30. A. M. P. C. Nunes, K. Zavitsanos, R. Del Conte, G. Malandrinos, N. Hadjiliadis. *Dalton Trans*. 1904 (2009).
31. A. M. Nunes, K. Zavitsanos, G. Malandrinos, N. Hadjiliadis. *Dalton Trans*. **39**, 4369 (2010).
32. A. M. Nunes, K. Zavitsanos, R. Del Conte, G. Malandrinos, N. Hadjiliadis. *Inorg. Chem.* **49**, 5658 (2010).
33. K. Zavitsanos, A. M. Nunes, G. Malandrinos, N. Hadjiliadis. *J. Inorg. Biochem.* **105**, 102 (2011).
34. A. Krezel, M. Mylonas, E. Kopera, W. Bal. *Acta Biochem. Pol*. **53**, 721 (2006).
35. E. Kopera, A. Krezel, A.-M. Protas, A. Belczyk, A. Bonna, A. Wystouch-Cieszynska, J. Poznanski, W. Bal. *Inorg. Chem.* **49**, 6636 (2010).
36. W. L. Cheung, K. Ajiro, K. Samejima, M. Kloc, P. Cheung, C. A. Mizzen, A. Beeser, L. D. Etkin, J. Chernoff, W. C. Earnshaw, C. D. Allis. *Cell* **113**, 507 (2003).
37. S. Y. Archer, R. A. Hodin. *Curr. Opin. Genet. Dev*. **9**, 171 (1999).
38. B. D. Strahl, C. D. Allis. *Nature* **403**, 41 (2000).
39. R. Nag, M. Kyriss, J. W. Smerdon, J. J. Wyrick, M. J. Smerdon. *Nucleic Acids Res*. **626**, 1450 (2010).

40. C. A. Davey, D. F. Sargent, K. Luger, A. W. Maeder, T. J. Richmond. *J. Mol. Biol.* **319**, 1097 (2002).
41. J. V. Chodaparambil, R. S. Edayathumangalam, Y. Bao, Y.-J. Park, K. Luger, in: S. L. Berger, O. Nakanishi, B. Haendler (Eds.). *Nucleosome Structure and Function, The Histone Code and Beyond: New Approaches to Cancer Therapy*, Springer, New York, **57**, 209 (2006).
42. S. D. Briggs, T. Xiao, Z. W. Sun, J. A. Caldwell, J. Shabanowitz, D. F. Hunt, C. D. Allis, B. D. Strahl. *Nature* **418**, 498 (2002).
43. K. Zavitsanos, A. M. Nunes, G. Malandrinos, N. Hadjiliadis. *J. Inorg. Biochem.* Accepted for publication.
44. M. A. Chevion. *Free Radical Biol. Med*. **5**, 27 (1988).
45. D. R. Lloyd, D. H. Phillips. *Mutat. Res*. **424**, 23 (1999).
46. W. Vogt. *Free Radical Biol. Med.* **18**, 93 (1995).
47. L. S. Nakao, L. K. Iwai, J. Kalil, O. Augusto. *FEBS Lett.* **547**, 87 (2003).

